Qualitative Analysis and Verification of Hybrid Models of Genetic Regulatory Networks: Nutritional Stress Response in *Escherichia coli*

Grégory Batt[1,2], Delphine Ropers[1], Hidde de Jong[1], Johannes Geiselmann[3], Michel Page[1,4], and Dominique Schneider[3]

[1] INRIA Rhône-Alpes, 655 avenue de l'Europe, Montbonnot, 38334 Saint Ismier Cedex, France
{Gregory.Batt, Delphine.Ropers, Hidde.de-Jong, Michel.Page}@inrialpes.fr
[2] Université Joseph Fourier, Grenoble, France
[3] Laboratoire Adaptation et Pathogénie des Microorganismes, CNRS UMR 5163, Université Joseph Fourier, Grenoble, France
{Hans.Geiselmann, Dominique.Schneider}@ujf-grenoble.fr
[4] Université Pierre Mendès France, Grenoble, France

Abstract. The switch-like character of the dynamics of genetic regulatory networks has attracted much attention from mathematical biologists and researchers on hybrid systems alike. We extend our previous work on a method for the qualitative analysis of hybrid models of genetic regulatory networks, based on a class of piecewise-affine differential equation (PADE) models, in two directions. First, we present a refinement of the method using a discrete or qualitative abstraction that preserves stronger properties of the dynamics of the PA systems, in particular the sign patterns of the derivatives of the concentration variables. The discrete transition system resulting from the abstraction is a conservative approximation of the dynamics of the PA system and can be computed symbolically. Second, we apply the refined method to a regulatory system whose functioning is not yet well-understood by biologists, the nutritional stress response in the bacterium *Escherichia coli*.

1 Introduction

The functioning and development of living organisms is controlled on the molecular level by networks of genes, proteins, small molecules, and their mutual interactions, so-called *genetic regulatory networks*. The dynamics of these networks is hybrid in nature, in the sense that the continuous evolution of the concentration of proteins and other molecules is punctuated by discrete changes in the activity of genes coding for the proteins. The switch-like character of the dynamics of genetic regulatory networks has attracted much attention from mathematical biologists and researchers on hybrid systems alike (*e.g.*, [1, 2, 3, 4, 5, 6, 7]).

While powerful techniques for the analysis, verification, and control of hybrid systems have been developed (see [8, 9] for reviews), the specificities of the

M. Morari and L. Thiele (Eds.): HSCC 2005, LNCS 3414, pp. 134–150, 2005.

biological application domain pose a number of challenges [10]. First, most genetic regulatory networks of interest consist of a large number of genes that are involved in complex, interlocked feedback loops. Second, the data available on both the structure and the dynamics of the systems is currently essentially qualitative in nature, meaning that numerical values for concentration variables and interaction parameters are generally absent. The above characteristics require hybrid-system methods and tools to be upscalable and capable of dealing with qualitative information.

In previous work [4, 11], we have developed a method for the *qualitative analysis of hybrid models of genetic regulatory networks*, using a class of piecewise-affine differential equation (PADE) models that has been well-studied in mathematical biology [1, 2] (see also [5]). The method is based on a qualitative abstraction of the dynamics of the PA systems and exploits favorable mathematical properties of the models to symbolically compute reachability properties. The method has been implemented in the publicly-available computer tool *Genetic Network Analysis (GNA)* [12] and validated on a well-understood network, the initiation of sporulation in *B. subtilis* [13].

The present paper extends our previous work in two directions. First, we present a refinement of the method using a qualitative abstraction that preserves stronger properties of the dynamics of the PA systems, in particular the sign patterns of the derivatives of the concentration variables. This information is critical for the experimental validation of models of genetic regulatory networks, since experimental measurements of the system dynamics by means of quantitative RT-PCR, reporter genes, and DNA microarrays usually result in observations of changes in the sign of derivatives. The refinement of the method, which has required us to deal with non-trivial technical difficulties arising from discontinuities in the righthand-side of the PADE models, has resulted in a new prototype version of the computer tool GNA. Second, we have applied the refined method to a biological system whose functioning is not yet well-understood by biologists, the nutritional stress response in the bacterium *E. coli*. This has led to new insights into how the adaptation of cell growth to nutritional stress emerges from the molecular interactions. Moreover, it has given rise to predictions of the behavior of the system after a nutrient upshift, which are currently being tested in our laboratory.

In Sections 2 and 3 of the paper, we review PADE models and their mathematical properties, with a special emphasis on a partition of the phase space preserving the sign of the derivatives of the concentration variables. This partition forms the basis for the definition, in Section 4, of a qualitative abstraction, transforming the continuous transition system associated with a PADE model into a discrete transition system. The discrete transition system is a simulation of the continuous transition system, thus providing a conservative approximation of the network dynamics. Moreover, the discrete transition system can be easily computed in a symbolic manner from inequality constraints on the parameters. In Section 5, we describe the application of the method to the qualitative anal-

ysis of the nutritional stress response in *E. coli*. The final section of the paper discusses the results in the context of related work on hybrid systems.[1]

2 PADE Models of Genetic Regulatory Networks

The dynamics of genetic regulatory networks can be modeled by a class of piecewise-affine differential equations (PADE) of the following general form [1, 2]:

$$\dot{\boldsymbol{x}} = \boldsymbol{h}(\boldsymbol{x}) = \boldsymbol{f}(\boldsymbol{x}) - \boldsymbol{g}(\boldsymbol{x})\,\boldsymbol{x}, \tag{1}$$

where $\boldsymbol{x} = (x_1, \ldots, x_n)' \in \Omega$ is a vector of cellular protein concentrations, $\boldsymbol{f} = (f_1, \ldots, f_n)'$, $\boldsymbol{g} = \mathrm{diag}(g_1, \ldots, g_n)$, and $\Omega \subset \mathbb{R}^n_{\geq 0}$ is a bounded n-dimensional phase space box. The rate of change of each protein concentration x_i, $1 \leq i \leq n$, is thus defined as the difference of the rate of synthesis $f_i(\boldsymbol{x})$ and the rate of degradation $g_i(\boldsymbol{x})\,x_i$ of the protein.

The function $f_i : \Omega \to \mathbb{R}_{\geq 0}$ expresses how the rate of synthesis of the protein encoded by gene i depends on the concentrations $\boldsymbol{x}$ of the proteins in the cell. More specifically, the function f_i is defined as

$$f_i(\boldsymbol{x}) = \sum_{l \in L_i} \kappa_i^l \, b_i^l(\boldsymbol{x}), \tag{2}$$

where $\kappa_i^l > 0$ is a rate parameter, $b_i^l : \Omega \to \{0, 1\}$ a piecewise-continuous *regulation function*, and L_i a possibly empty set of indices of regulation functions. The function g_i expresses the regulation of protein degradation. It is defined analogously to f_i, except that we demand that g_i is strictly positive. In addition, in order to formally distinguish degradation rate parameters from synthesis rate parameters, we will denote the former by γ instead of κ. Notice that with the above definitions, $\boldsymbol{h}$ is a *piecewise-affine (PA)* vector-valued function.

A regulation function b_i^l describes the conditions under which the protein encoded by gene i is synthesized (degraded) at a rate κ_i^l ($\gamma_i^l\,x_i$). It is defined in terms of step functions and is the arithmetic equivalent of a Boolean function expressing the logic of gene regulation [1, 2]. More precisely, the conditions for synthesis or degradation are expressed using the step functions s^+, s^-:

$$s^+(x_j, \theta_j) = \begin{cases} 1, \text{ if } x_j > \theta_j, \\ 0, \text{ if } x_j < \theta_j, \end{cases} \text{ and } s^-(x_j, \theta_j) = 1 - s^+(x_j, \theta_j). \tag{3}$$

where x_j is an element of the state vector $\boldsymbol{x}$ and θ_j a constant denoting a threshold concentration.

Figure 1(a) gives an example of a simple genetic regulatory network consisting of two genes, a and b. When a gene (a or b) is expressed, the corresponding protein (A or B) is synthesized at a specified rate (κ_a or κ_b). Proteins A and B

[1] A detailed description of the method and the proofs of the propositions can be found in [14].

regulate the expression of genes a and b. More specifically, protein B inhibits the expression of gene a, above a certain threshold concentration θ_b, while protein A inhibits the expression of gene b above a threshold concentration θ_a^1, and the expression of its own gene above a second, higher threshold concentration θ_a^2. The degradation of the proteins is not regulated and therefore proportional to the concentration of the proteins (with degradation parameters γ_a or γ_b).

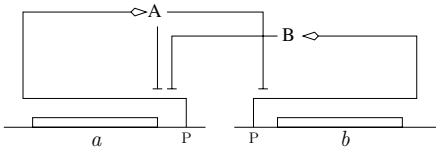

(a)

$$\dot{x}_a = \kappa_a\, s^-(x_a, \theta_a^2)\, s^-(x_b, \theta_b) - \gamma_a\, x_a,$$
$$\dot{x}_b = \kappa_b\, s^-(x_a, \theta_a^1) - \gamma_b\, x_b.$$

(b)

Fig. 1. (a) Example of a genetic regulatory network of two genes (a and b), each coding for a regulatory protein (A and B). For legend, see Figure 4. (b) PADE model corresponding to the network in (a)

The use of step functions $s^{\pm}(x_j, \theta_j)$ in (1) gives rise to complications, because the step functions are discontinuous at $x_j = \theta_j$, and therefore $\boldsymbol{h}$ is discontinuous on $\Theta = \bigcup_{i\in[1..n], l_i\in[1..p_i]}\{\boldsymbol{x} \in \Omega \mid x_i = \theta_i^{l_i}\}$, the union of the threshold hyperplanes (where the protein encoded by gene i is assumed to have p_i threshold concentrations). In order to deal with this problem, we can follow an approach widely used in control theory, originally proposed by Filippov [15]. It consists in extending the differential *equation* $\dot{\boldsymbol{x}} = \boldsymbol{h}(\boldsymbol{x})$, $\boldsymbol{x} \in \Omega \setminus \Theta$, to the differential *inclusion*

$$\dot{\boldsymbol{x}} \in K(\boldsymbol{x}), \text{ with } K(\boldsymbol{x}) = \overline{co}(\{\lim_{\boldsymbol{y}\to\boldsymbol{x},\, \boldsymbol{y}\notin\Theta} \boldsymbol{h}(\boldsymbol{y})\}),\ \boldsymbol{x} \in \Omega, \tag{4}$$

where $\overline{co}(P)$ denotes the smallest closed convex set containing the set P and $\{\lim_{\boldsymbol{y}\to\boldsymbol{x},\, \boldsymbol{y}\notin\Theta} \boldsymbol{h}(\boldsymbol{y})\}$, the set of all limit values of $\boldsymbol{h}(\boldsymbol{y})$, for $\boldsymbol{y} \notin \Theta$ and $\boldsymbol{y} \to \boldsymbol{x}$. This approach has been applied in the context of genetic regulatory network modeling by Gouzé and Sari [16].

In practice, $K(\boldsymbol{x})$ may be difficult to compute because the smallest closed convex set can be a complex polyhedron in Ω. We therefore employ an alternative extension of the differential equation:

$$\dot{\boldsymbol{x}} \in H(\boldsymbol{x}), \text{ with } H(\boldsymbol{x}) = \overline{rect}(\{\lim_{\boldsymbol{y}\to\boldsymbol{x},\, \boldsymbol{y}\notin\Theta} \boldsymbol{h}(\boldsymbol{y})\}),\ \boldsymbol{x} \in \Omega, \tag{5}$$

where $\overline{rect}(P)$ denotes the smallest closed *hyperrectangular* set containing the set P [11, 14]. The advantage of using $\overline{rect}$ is that we can rewrite $H(\boldsymbol{x})$ as a system of differential inclusions $\dot{x}_i \in H_i(\boldsymbol{x})$, $i \in [1..n]$. Notice that $H(\boldsymbol{x})$ is an overapproximation of $K(\boldsymbol{x})$, for all $\boldsymbol{x} \in \Omega$.

Formally, we define the *PA system* Σ as the triple (Ω, Θ, H), that is, the set-valued function H given by (5), defined on the n-dimensional phase space

Ω, with Θ the union of the threshold hyperplanes. A *solution* of the PA system Σ on a time interval I is a solution of the differential inclusion (5) on I, that is, an absolutely-continuous vector-valued function $\boldsymbol{\xi}(t)$ such that $\dot{\boldsymbol{\xi}}(t) \in H(\boldsymbol{\xi}(t))$ almost everywhere on I. In particular, $\dot{\boldsymbol{\xi}}(t) \in H(\boldsymbol{\xi}(t))$ may not hold, if $\boldsymbol{\xi}$ reaches or leaves Ω at t.

For all $\boldsymbol{x}_0 \in \Omega$ and $\tau \in \mathbb{R}_{>0} \cup \{\infty\}$, $\Xi^{\omega}_{\Sigma}(\boldsymbol{x}_0, \tau)$ will denote the set of solutions $\boldsymbol{\xi}(t)$ of the PA system Σ, for the initial condition $\boldsymbol{\xi}(0) = \boldsymbol{x}_0$, and $t \in [0, \tau]$, if τ is finite, or $[0, \infty)$, otherwise.[2] Since the right-hand side of (5) is upper semicontinuous, the existence of at least one solution $\boldsymbol{\xi}$ on some time interval $[0, \tau]$, $\tau > 0$, with initial condition $\boldsymbol{\xi}(0) = \boldsymbol{x}_0$ is guaranteed for all $\boldsymbol{x}_0$ in Ω [15]. However, there is, in general, not a unique solution. The set $\Xi^{\omega}_{\Sigma} = \bigcup_{\boldsymbol{x}_0 \in \Omega, \tau > 0} \Xi^{\omega}_{\Sigma}(\boldsymbol{x}_0, \tau)$ is the set of all solutions, on a finite or infinite time interval, of the PA system Σ. We restrict our analysis to the set Ξ_{Σ} of the solutions in Ξ^{ω}_{Σ} that reach and leave a threshold hyperplane finitely-many times.

3 Mathematical Analysis of PA Systems

The dynamical properties of the solutions of Σ can be analyzed in the n-dimensional phase space box $\Omega = \Omega_1 \times \ldots \times \Omega_n$, where $\Omega_i = \{x_i \in \mathbb{R} \mid 0 \leq x_i \leq max_i\}$ and max_i denotes a maximum concentration of each protein, $1 \leq i \leq n$. The $(n-1)$-dimensional threshold hyperplanes $\{\boldsymbol{x} \in \Omega \mid x_i = \theta_i^{l_i}\}$, $1 \leq l_i \leq p_i$, $1 \leq i \leq n$, partition Ω into (hyper)rectangular regions. Since the regulation of gene expression is identical everywhere in such a region (see below), it corresponds to a regulatory *mode*. Consequently, the regions are called *mode domains*. The set of mode domains of Ω is referred to as $\mathcal{M}$.

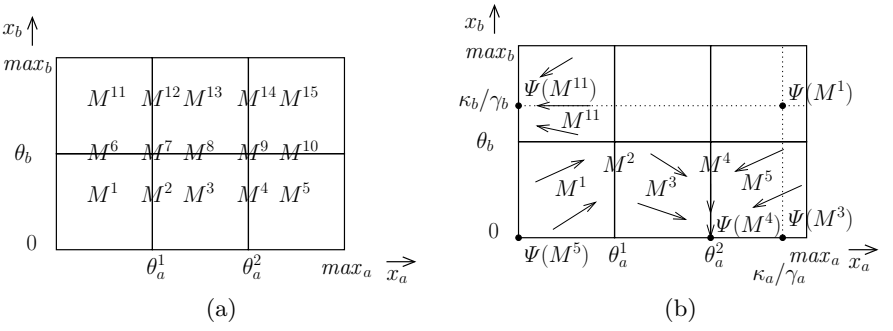

Fig. 2. (a) Partition by mode domains of the phase space corresponding to the model of Figure 1(b). (b) Focal sets and dynamics of the mode domains M^1 to M^5, and M^{11}

[2] In the sequel, we say, by abuse of terminology, that $\boldsymbol{\xi}$ is a solution of Σ on $[0, \tau]$, $\tau \in \mathbb{R}_{>0} \cup \{\infty\}$.

Figure 2(a) shows the partitioning into mode domains of the two-dimensional phase space of the example network. We distinguish between mode domains like M^7 and M^2, which are located on (intersections of) threshold hyperplanes, and mode domains like M^1, which are not. The former domains are called *singular* mode domains and the latter *regular* mode domains. We denote by $\mathcal{M}_r$ and $\mathcal{M}_s$ the sets of regular and singular mode domains, respectively.

We introduce some simple topological concepts. For every hyperrectangular region, $R \subseteq \Omega$, of dimension k, $0 \leq k \leq n$, we define the supporting hyperplane of R, $supp(R) \subseteq \Omega$, as the k-dimensional hyperplane containing R. The boundary of R in $supp(R)$ is denoted by ∂R. Suppose that M is a singular mode domain, *i.e.* $M \in \mathcal{M}_s$. Then $R(M)$ is defined as the set of regular mode domains M' having M in their boundary, *i.e.* $R(M) = \{M' \in \mathcal{M}_r \mid M \subseteq \partial M'\}$.

Using the definition of the differential inclusion (5), it can be easily shown that in a regular mode domain M, $H(\boldsymbol{x})$ reduces to the singleton set $\{\boldsymbol{\mu}^M - \boldsymbol{\nu}^M \boldsymbol{x}\}$, for all $\boldsymbol{x} \in M$, where $\boldsymbol{\mu}^M$ is a vector of (sums of) synthesis rate constants and $\boldsymbol{\nu}^M$ a diagonal matrix of (sums of) degradation rate constants. This yields the classical result that all solutions $\boldsymbol{\xi}$ in M monotonically converge towards the *focal set* $\Psi(M) = \{\boldsymbol{\psi}(M)\}$, where $\boldsymbol{\psi}(M) = (\boldsymbol{\nu}^M)^{-1}\boldsymbol{\mu}^M$ [1]. We will make the generic assumption that the focal sets $\Psi(M)$, for all $M \in \mathcal{M}_r$, are not located in the threshold hyperplanes Θ. Figure 2(b) shows the focal sets of four regular mode domains (M^1, M^3, M^5 and M^{11}). In the case of M^{11}, we see that $\Psi(M^{11}) \subseteq M^{11}$, so that $\psi(M^{11})$ is an asymptotically stable equilibrium point of Σ.

In a singular mode domain, the right-hand side of the differential inclusion (5) reduces to $H(\boldsymbol{x}) = \overline{rect}(\{\boldsymbol{\mu}^{M'} - \boldsymbol{\nu}^{M'}\boldsymbol{x} \mid M' \in R(M)\})$, for all $\boldsymbol{x} \in M$ [11, 16]. The focal set associated with the domain now becomes $\Psi(M) = supp(M) \cap \overline{rect}(\{\boldsymbol{\psi}(M') \mid M' \in R(M)\})$, which is generally not a single point in higher-dimensional domains [11, 16]. Two different cases can be distinguished. If $\Psi(M)$ is empty, then every solution passes through M instantaneously [16] and M is called an *instantaneous* mode domain. If not, then some (but not necessarily all) solutions arriving at M will remain in M for some time, sliding along the threshold planes containing M [16]. M is then called *persistent*. If $\Psi(M)$ is a single point, then all solutions in M monotonically converge towards this point. In the case that $\Psi(M)$ is not a single point, a weaker monotonicity property holds [11, 16]. Figure 2(b) shows two singular mode domains, M^2 and M^4. M^2 is an instantaneous mode domain ($\Psi(M^2) = \emptyset$), whereas M^4 is a persistent mode domain in which solutions slide along the threshold plane. In this simple example, it is intuitively clear how to define the flow in M^4, given the dynamics in M^3 and M^5. The use of differential inclusions as described above makes it possible to define the flow in singular domains in a systematic and mathematically proper way.

The fact that every mode domain is associated with a unique focal set has provided the basis for the abstraction criterion employed in our previous work [4, 11]. However, this criterion disregards that the system does not always exhibit the same qualitative dynamics in different parts of a mode domain, in the

sense that the sign pattern of the derivatives of the solutions $\boldsymbol{\xi}$ may not be unique. Consider the case of M^{11} in Figure 2(b): depending on whether $\xi_b(t)$ is above, on, or below the focal concentration κ_b/γ_b in M^{11}, ξ_b will be decreasing, steady, or increasing. As a consequence, if we abstract the domain M^{11} away in a single discrete state, we will not be able to unambiguously infer that solutions entering this domain from M^6 are increasing in the x_b-dimension. This may lead to problems when comparing predictions from the model with gene expression data, for instance the observed variation of the sign of x_b. Today's experimental techniques, such as quantitative RT-PCR, reporter genes, and DNA microarrays, usually produce information on changes in the sign of the derivatives of the concentration variables.

The mismatch between the abstraction levels of the mathematical analysis and the experimental data calls for a finer partitioning of the phase space, which can then provide the basis for a more adequate abstraction criterion. Along these lines, the regular and singular mode domains distinguished above are repartitioned into (hyper)rectangular regions called *flow domains*. In the case that a mode domain M is regular, it is split by the $(n-1)$-dimensional hyperplanes $\{\boldsymbol{x} \in \Omega \mid x_i = \psi_i(M)\}$, $i \in [1..n]$, that intersect with M. Under the same condition, singular mode domains M are repartitioned by the $(n-1)$-dimensional hyperplanes $\{\boldsymbol{x} \in \Omega \mid x_i = \psi_i(M')\}$, $M' \in R(M)$, $i \in [1..n]$. The resulting set of flow domains is denoted by $\mathcal{D}$ [14]. The partitioning of the phase space into 27 flow domains is illustrated for the example system in Figure 3(a). Every flow domain is included in a single mode domain, a relation captured by the surjective function *mode*: $\mathcal{D} \to \mathcal{M}$, defined as $mode(D) = M$, iff $D \subseteq M$. Similarly, the function *flow*: $\Omega \to \mathcal{D}$ denotes the surjective mapping that associates a point in the phase space to its flow domain: $flow(\boldsymbol{x}) = D$, iff $\boldsymbol{x} \in D$.

The repartitioning of mode domain M^{11} leads to six flow domains (Figure 3(a)). The finer partition guarantees that in every flow domain of M^{11}, the derivatives have a unique sign pattern. In $D^{11.2}$, for instance, the x_a-derivative is negative and the x_b-derivative is positive, whereas in $D^{11.3}$ both derivatives equal zero (in fact, $D^{11.3}$ coincides with $\boldsymbol{\psi}(M^{11})$ and is an equilibrium point of the system). The above property is true more generally. Consider a point $\boldsymbol{x}$ in a flow domain $D \in \mathcal{D}$. We denote by $S(\boldsymbol{x}) \in 2^{\{-1,0,1\}^n}$ the set of derivative sign vectors of the solutions in D passing through $\boldsymbol{x}$, that is, $S(\boldsymbol{x}) = \{\boldsymbol{sign}(\dot{\boldsymbol{\xi}}(t_x)) \mid \boldsymbol{\xi} \in \Xi_\Sigma \text{ in } D,\ \boldsymbol{\xi}(t_x) = \boldsymbol{x},\ \text{and } \dot{\boldsymbol{\xi}}(t_x) \in H(\boldsymbol{\xi}(t_x))\}$. Notice that the definition of S as a set is a direct consequence of the use of differential inclusions. Theorem 1 states that $S(\boldsymbol{x})$ is the same for every $\boldsymbol{x} \in D$.

Theorem 1 (Qualitatively-identical dynamics in flow domain). For all $D \in \mathcal{D}$, for all $\boldsymbol{x}, \boldsymbol{x}' \in D$, $S(\boldsymbol{x}) = S(\boldsymbol{x}')$.

The theorem suggests that the partition of the phase space introduced in this section can be used as an abstraction criterion better-adapted to the available experimental data on gene expression. This idea will be further developed in the next section.

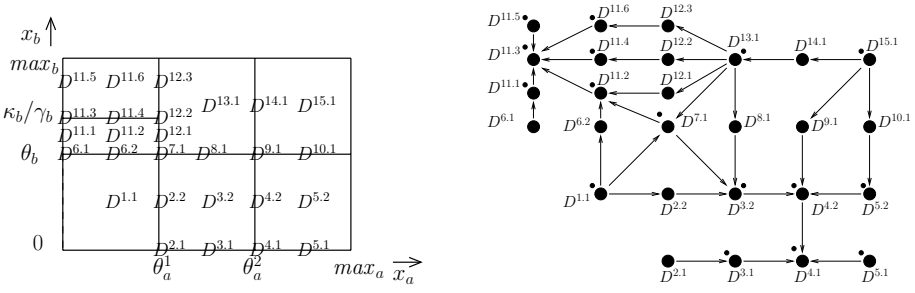

(c) $0 < \theta_a^1 < \theta_a^2 < \kappa_a/\gamma_a < max_a$ and $0 < \theta_b < \kappa_b/\gamma_b < max_b$

Fig. 3. (a) Partition by flow domains of the phase space of the model in Figure 1(b). (b) State transition graph of the corresponding qualitative transition system. For the sake of clarity, self-transitions are represented by dots and transition labels are omitted. (c) Inequality constraints on parameters for which the graph in (b) is obtained

4 Qualitative Abstraction of the Dynamics of PA Systems

As a preparatory step, we define a *continuous transition system* having the same reachability properties as the original PA system Σ. Consider $\boldsymbol{x} \in D$ and $\boldsymbol{x'} \in D'$, where $D, D' \in \mathcal{D}$ are flow domains. If there exists a solution $\boldsymbol{\xi}$ of Σ passing through $\boldsymbol{x}$ at time $\tau \in \mathbb{R}_{\geq 0}$ and reaching $\boldsymbol{x'}$ at time $\tau' \in \mathbb{R}_{>0} \cup \{\infty\}$, without leaving $D \cup D'$ in the time interval $[\tau, \tau']$, then the absolute continuity of $\boldsymbol{\xi}$ implies that D and D' are either equal or contiguous. More precisely, one of the three following cases holds: $D = D'$, $D \in \partial D'$, or $D' \in \partial D$. We consequently distinguish three types of continuous transition that correspond to these three cases: *internal*, denoted by $\boldsymbol{x} \xrightarrow{int} \boldsymbol{x'}$, *dimension increasing*, denoted by $\boldsymbol{x} \xrightarrow{dim^+} \boldsymbol{x'}$, and *dimension decreasing*, denoted by $\boldsymbol{x} \xrightarrow{dim^-} \boldsymbol{x'}$. The latter two terms refer to the increase or decrease in dimension when going from D to D'. This leads to the following definition:

Definition 1 (PA transition system). Σ-TS $= (\Omega, L, \Pi, \rightarrow, \models)$ is the transition sytem corresponding to the PA system $\Sigma = (\Omega, \Theta, H)$, where:

- Ω is the state space;
- $L = \{int, dim^+, dim^-\}$ is a set of labels denoting the three different types of transitions;
- $\Pi = \{Dsign = S \mid S \in 2^{\{-1,0,1\}^n}\}$ is a set of propositions describing the signs of the derivatives of the concentration variables;
- $\rightarrow$ is the transition relation describing the continuous evolution of the system, defined by $\rightarrow \subseteq \Omega \times L \times \Omega$, such that $\boldsymbol{x} \xrightarrow{l} \boldsymbol{x'}$ iff there exists $\boldsymbol{\xi} \in \Xi_\Sigma$ and τ, τ', such that $0 \leq \tau < \tau'$, $\boldsymbol{\xi}(\tau) = \boldsymbol{x}$, $\boldsymbol{\xi}(\tau') = \boldsymbol{x'}$, and

  - if $l = int$, then for all $t \in [\tau, \tau']$: $\boldsymbol{\xi}(t) \in \mathit{flow}(\boldsymbol{x}) = \mathit{flow}(\boldsymbol{x'})$,
  - if $l = dim^+$, then for all $t \in (\tau, \tau']$: $\boldsymbol{\xi}(t) \in \mathit{flow}(\boldsymbol{x'}) \neq \mathit{flow}(\boldsymbol{x})$,
  - if $l = dim^-$, then for all $t \in [\tau, \tau')$: $\boldsymbol{\xi}(t) \in \mathit{flow}(\boldsymbol{x}) \neq \mathit{flow}(\boldsymbol{x'})$;
- $\models$ is the satisfaction relation of the propositions in Π, defined by $\models \subseteq \Omega \times \Pi$, such that $\boldsymbol{x} \models \mathit{Dsign} = S$ iff $S = S(\boldsymbol{x})$.

The satisfaction relation $\models$ thus associates to each point $\boldsymbol{x}$ in the phase space a qualitative description of the dynamics of the system at $\boldsymbol{x}$. We define any sequence of points in Ω, $(\boldsymbol{x}^0, \ldots, \boldsymbol{x}^m)$, $m \geq 0$, as a *run* of Σ-TS if for all $i \in [0..m\text{–}1]$, there exists some $l \in L$ such that $\boldsymbol{x}^i \xrightarrow{l} \boldsymbol{x}^{i+1}$. It is not difficult to show that a PA system Σ and its corresponding PA transition system Σ-TS have equivalent reachability properties (see Theorem 2 in [14]).

The continuous PA transition system has an infinite number of states and transitions, as a consequence of which conventional tools for model checking cannot be used to verify properties of the system. However, we can define a discrete transition system, with a finite number of states and transitions, that preserves important properties of the qualitative dynamics of the system. In order to achieve this, we introduce the equivalence relation $\sim_\Omega \subseteq \Omega \times \Omega$ induced by the partition $\mathcal{D}$ of the phase space: $\boldsymbol{x} \sim_\Omega \boldsymbol{x'}$ iff $\mathit{flow}(\boldsymbol{x}) = \mathit{flow}(\boldsymbol{x'})$. From Theorem 1 it follows that $\sim_\Omega$ is *proposition-preserving* [17, 18], in the sense that for all $\boldsymbol{x}, \boldsymbol{x'} \in D$ and for all $\pi \in \Pi$, $\boldsymbol{x} \models \pi$ iff $\boldsymbol{x'} \models \pi$.

The discrete or *qualitative abstraction* of a PA transition system Σ-TS, called *qualitative PA transition system*, is now defined as the quotient transition system of Σ-TS, given the equivalence relation $\sim_\Omega$ [17, 18].

Definition 2 (Qualitative PA transition system). The qualitative PA transition system corresponding to the PA transition system Σ-TS $= (\Omega, L, \Pi, \rightarrow, \models)$ is Σ-QTS $= (\Omega/_{\sim_\Omega}, L, \Pi, \rightarrow_{\sim_\Omega}, \models_{\sim_\Omega})$.

Proposition 1 (Qualitative PA transition system). Let Σ-QTS $= (\Omega/_{\sim_\Omega}$, L, $\Pi, \rightarrow_{\sim_\Omega}, \models_{\sim_\Omega})$ be the qualitative PA transition system corresponding to the PA transition system Σ-TS $= (\Omega, L, \Pi, \rightarrow, \models)$. Then

- $\Omega/_{\sim_\Omega} = \mathcal{D}$;
- $\rightarrow_{\sim_\Omega} \subseteq \mathcal{D} \times L \times \mathcal{D}$, such that $D \xrightarrow{l}_{\sim_\Omega} D'$ iff $\exists \boldsymbol{\xi} \in \Xi_\Sigma, \exists \tau, \tau',\ 0 \leq \tau < \tau'$ such that $\boldsymbol{\xi}(\tau) \in D$, $\boldsymbol{\xi}(\tau') \in D'$, and
  - if $l = int$, then for all $t \in [\tau, \tau']$: $\boldsymbol{\xi}(t) \in D = D'$,
  - if $l = dim^+$, then for all $t \in (\tau, \tau']$: $\boldsymbol{\xi}(t) \in D' \neq D$,
  - if $l = dim^-$, then for all $t \in [\tau, \tau')$: $\boldsymbol{\xi}(t) \in D \neq D'$;
- $\models_{\sim_\Omega} \subseteq \mathcal{D} \times \Pi$, such that $D \models \mathit{Dsign} = S$ iff $\forall \boldsymbol{x} \in D$: $S(\boldsymbol{x}) = S$.

Notice that the transitions labeled by dim^+ or dim^- connect two different flow domains, since in Proposition 1 we require that $D \neq D'$. This corresponds to a continuous evolution of the system along which it switches from one flow domain to another. On the contrary, the transitions labeled by *int* correspond to the continuous evolution of the system in a single flow domain. Notice also that qualitative PA transition systems are non-deterministic.

As for Σ-TS, we define any sequence of flow domains $(D^0, \ldots, D^m)$, $m \geq 0$, as a *run* of Σ-QTS iff for all $i \in [0..m\text{–}1]$, there exists $l \in L$ such that $D^i \xrightarrow{l}_{\sim_\Omega} D^{i+1}$. The satisfaction relation $\models_{\sim_\Omega}$ associates to every run a qualitative description of the evolution of the derivatives over time. Σ-QTS can be represented by a directed graph $G = (\mathcal{D}, \rightarrow_{\sim_\Omega})$, called the *state transition graph*. The paths in G represent the runs of the system. The state transition graph corresponding to the two-gene example is represented in Figure 3(b), and $(D^{1.1}, D^{2.2}, D^{3.2}, D^{4.2}, D^{4.1})$ is an example of a run.

It directly follows from the definitions of quotient transition system and simulation of transition systems [17, 18] that Σ-QTS is a *simulation* of Σ-TS. The converse is not true in general, so that Σ-QTS and Σ-TS are not bisimilar.

Proposition 2. Σ-QTS is a simulation of Σ-TS.

As a consequence of Proposition 2, if there exists a run $(\boldsymbol{x}^0, \ldots, \boldsymbol{x}^m)$ of Σ-TS, then there also exists a run $(D^0, \ldots, D^m)$ of Σ-QTS such that $\boldsymbol{x}^i \in D^i$, for all $i \in [0..m]$. In other words, Σ-QTS is a *conservative approximation* of Σ-TS.

In [14] we introduce a second equivalence relation $\sim_\Gamma \subseteq \Gamma \times \Gamma$, defined on the parameter space Γ of the PA system. Two parameter vectors $\boldsymbol{p}$ and $\boldsymbol{p'}$ are equivalent, if their corresponding qualitative PA transition systems, and hence the state transition graphs, are isomorphic. We show that a certain class of parameter inequality constraints define regions $P \subseteq \Gamma$, such that for every $\boldsymbol{p}, \boldsymbol{p'} \in P$, it holds that $\boldsymbol{p} \sim_\Gamma \boldsymbol{p'}$. More precisely, there exists some $Q \in \Gamma/_{\sim_\Gamma}$, such that $P \subseteq Q$ (Theorem 3 in [14]). As a consequence, for all vectors of parameter values satisfying the inequality constraints, the system has the same qualitative dynamics. Whereas exact numerical values for the parameters are usually not available, the weaker information required for the formulation of the inequality constraints can often be obtained from the experimental literature, as illustrated in Section 5. Figure 3(c) shows the inequality constraints for which the state transition graph of our example is obtained.

The inequality constraints also play a key role in the actual computation of the qualitative PA transition system Σ-QTS [14]. The computation of Σ-QTS is greatly simplified by the fact that the domains D and the focal sets $\Psi(M)$ are hyperrectangular sets, which allows them to be expressed as product sets, *i.e.* $D = D_1 \times \ldots \times D_n$ and $\Psi(M) = \Psi_1(M) \times \ldots \times \Psi_n(M)$. As a consequence, the computation can be carried out for each dimension separately. For instance, the repartitioning of mode domain D^{11} into flow domains (Figure 3(a)) is based on the fact that the x_a-component $[0, \theta_a^1)$ is partitioned into two subsets by the segment $x_a = 0$, and the x_b-component $(\theta_b, max_b]$ into three subsets by the segment $x_b = \kappa_b/\gamma_b$. The product of these subsets yields the six flow domains shown in the figure. Notice also that, in order to derive this result, we only need to know the ordering of θ_a^1 and κ_a/γ_a in the x_a-dimension, and that of θ_b and κ_b/γ_b in the x_b-dimension, which are fixed by the inequality constraints in Figure 3(c). This result is true more generally and also applies to the transition relation $\rightarrow_{\sim_\Omega}$ and the satisfaction relation $\models_{\sim_\Omega}$. That is, the domains, the transitions, and the sign pattern of the derivatives can be straightforwardly derived by means

of symbolic computation using the inequality constraints. The algorithms are described in more detail in [14] and have been implemented in a new prototype version of the computer tool *GNA* [12]. The state transition graph generated by GNA can be exported to standard model-checking tools like NuSMV and CADP [22].

5 Application: Qualitative Analysis of Nutritional Stress Response in *E. coli*

In case of nutritional stress, an *Escherichia coli* population abandons exponential growth and enters a non-growth state called *stationary phase*. This growth-phase transition is accompanied by numerous physiological changes in the bacteria, concerning among other things the morphology and the metabolism of the cell, as well as gene expression [19]. On the molecular level, the transition from exponential phase to stationary phase is controlled by a complex genetic regulatory network integrating various environmental signals. The molecular basis of the adaptation of the growth of *E. coli* to nutritional stress conditions has been the focus of extensive studies for decades [20]. However, notwithstanding the enormous amount of information accumulated on the genes, proteins, and other molecules known to be involved in the stress adaptation process, there is currently no global understanding of how the response of the cell emerges from the network of molecular interactions. Moreover, with some exceptions, numerical values for the parameters characterizing the interactions and the molecular concentrations are absent, which makes it difficult to apply traditional methods for the dynamical modeling of genetic regulatory networks.

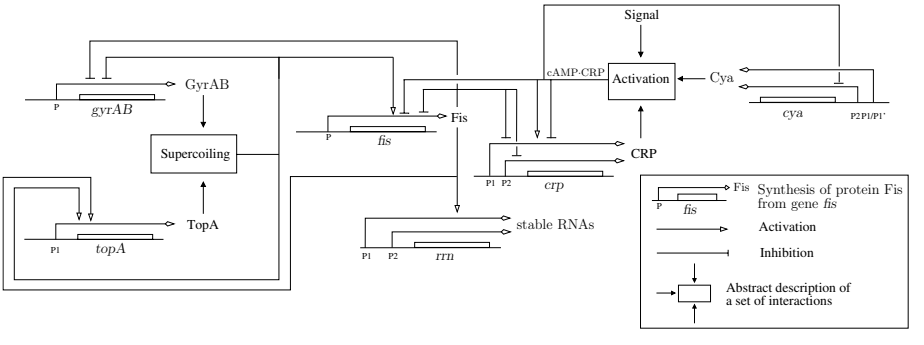

Fig. 4. Network of key genes, proteins, and regulatory interactions involved in the nutritional stress network in *E. coli*. The contents of the boxes labelled 'Activation' and 'Supercoiling' are detailed in [21]

The above circumstances have motivated the qualitative analysis of the nutritional stress response network in *E. coli* by means of the method presented in this paper [21]. On the basis of literature data, we have decided to focus, as

a first step, on a network of six genes that are believed to play a key role in the nutritional stress response (Figure 4). The network includes genes involved in the transduction of the nutritional stress signal (the global regulator *crp* and the adenylate cyclase *cya*), metabolism (the global regulator *fis*), cellular growth (the *rrn* genes coding for stable RNAs), and DNA supercoiling, an important modulator of gene expression (the topoisomerase *topA* and the gyrase *gyrAB*).

Based on this information, a PADE model of seven variables has been constructed, one protein concentration variable for each of the six genes and one input variable (u_{signal}) representing the presence or absence of a nutritional stress signal [21]. As an illustration, the piecewise-affine differential equation and the parameter inequality constraints for the state variable x_{topA} are given below.

$$\dot{x}_{topA} = \kappa^1_{topA} + \kappa^2_{topA}\, s^+(x_{gyrAB}, \theta^3_{gyrAB})\, s^-(x_{topA}, \theta^1_{topA})\, s^+(x_{fis}, \theta^4_{fis}) - \gamma_{topA}\, x_{topA}$$

$$0 < \kappa^1_{topA}/\gamma_{topA} < \theta^1_{topA} < \theta^2_{topA} < \theta^3_{topA} < (\kappa^1_{topA} + \kappa^2_{topA})/\gamma_{topA} < max_{topA}$$

The above equation and inequalities state that the basal expression of *topA* is low ($\kappa^1_{topA}/\gamma_{topA} < \theta^1_{topA}$), whereas in the presence of a high concentration of Fis ($s^+(x_{fis}, \theta^4_{fis}) = 1$), and of a low level of DNA supercoiling ($s^+(x_{gyrAB}, \theta^3_{gyrAB})$ $s^-(x_{topA}, \theta^1_{topA}) = 1$), the concentration of TopA increases, converging towards a high value ($(\kappa^1_{topA} + \kappa^2_{topA})/\gamma_{topA} > \theta^3_{topA}$).

Using the computer tool GNA, we have performed reachability analyses on the qualitative PA transition system associated with the PADE model. The simulation of the entry into stationary phase has given rise to a state transition graph of 712 states, computed in 5.0 s on a PC (800 MHz, 256 Mb). Figure 5 represents the temporal evolution of two of the protein concentrations in a run. The evolutions are consistent with the observations [21]. The coupling of GNA with model-checking tools [22] has allowed a more systematic verification of observed dynamical properties.

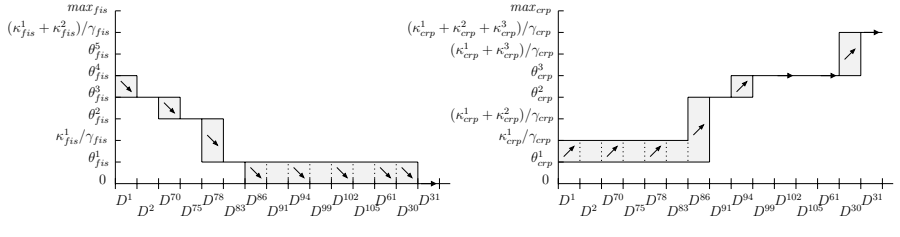

Fig. 5. Temporal evolution of Fis and CRP concentrations in the run $(D^1, \ldots, D^{31})$. Arrows indicate the sign of the derivative for persistent states

The application of the method has led to new insights into how the nutritional stress signal results in the slowing-down of bacterial growth characteristic for the stationary phase [21]. In summary, the analysis has brought to the fore

the role of the mutual inhibition of Fis and CRP, which in the presence of a nutritional stress signal results in the inhibition of *fis* and in the activation of *crp*. This causes a decrease of the expression of the *rrn* genes, which code for stable RNAs and are a reliable indicator of cellular growth. In addition to this increased understanding of the transition from exponential to stationary phase, the model has yielded predictions on the occurrence of oscillations in some of the protein concentrations after a nutrient upshift, predictions that are currently being tested in our laboratory. The scope of our study is now being enlarged to more complex nutritional stress response networks.

The analysis of the nutritional stress response in *E. coli* has confirmed the utility of the refined qualitative abstraction presented in this paper. Repartitioning the mode domains, such that the sign patterns of the derivatives of the concentration variables in the states of the qualitative PA transition system are unique, avoids verification of dynamical properties to be over-conservative. Consider Figure 6, which compares two-dimensional projections of a phase-space slice of the stress response model. Depending on whether mode domains or flow domains are used as the abstraction criterion, the state transition graph will be different (compare (d) and (e) of Figure 6). Whereas the CTL formula $EF(\dot{x}_{crp} > 0 \wedge EF\ (\dot{x}_{crp} < 0))$ holds for the graph in (d), this is not true in (e), thus revealing that the coarse-grained abstraction may cause models to escape refutation by available experimental data.

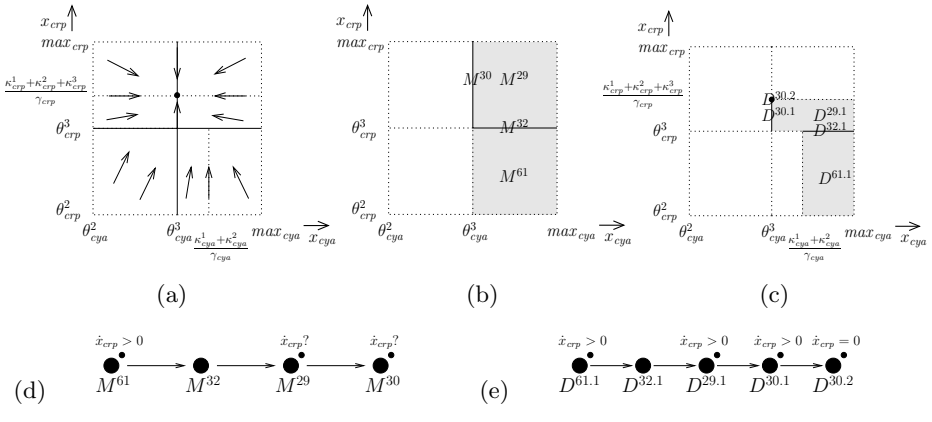

Fig. 6. (a) Two-dimensional projection of a slice of the phase space of the *E. coli* stress response model for the variables x_{crp} and x_{cya}. (b)-(c) Partitioning into (b) mode domains and (c) flow domains of the projection. (d)-(e) Excerpts of state transition graph resulting from the qualitative abstraction based on (d) mode domains and (e) flow domains

The application of the fine-grained qualitative abstraction to the nutritional stress response system has also revealed that it is not much more computationally-expensive than the coarse-grained abstraction used in our previous work. In fact,

when analyzing the transition from exponential to stationary phase, the refined abstraction generates 712 persistent states, whereas the original qualitative PA transition system has 39 persistent states. However, when defining a single initial state, corresponding to the biologically most plausible flow domain after repartitioning of the mode domain, the refined abstraction yields only 40 persistent states. A more systematic study of a PADE model with nine state and two input variables, describing the initiation of sporulation in *B. subtilis* for the wild-type and a dozen of mutant strains, confirms this result. On average, the refined abstraction generates only twice as much states, under the condition that the reachability analysis is carried out from a single flow domain.

6 Discussion and Conclusions

We have presented a method for the qualitative analysis and verification of hybrid models of genetic regulatory networks. The method is based on a class of piecewise-affine differential equation models that has been well-studied in mathematical biology. By defining a qualitative abstraction preserving the sign pattern of the derivatives of concentration variables, the continuous PA transition system associated with a PADE model is transformed into a discrete or qualitative PA transition system whose properties can be analyzed by means of classical model-checking tools. The qualitative PA transition is a simulation of the underlying continuous PA transition system and can be easily computed in a symbolic manner by exploiting inequality constraints on the parameters.

The results of this paper extend our previous work [4, 11] in two directions. In the first place, we have defined a refined partitioning of the phase space which underlies a qualitative abstraction preserving stronger properties of the qualitative dynamics of the system, *i.e.* the derivative sign pattern. The resulting qualitative PA transition system is better adapted to the abstraction level of the experimental data, in the sense that it avoids verification of dynamical properties to be over-conservative. In the second place, we have applied the implementation of the method to the analysis of a system whose functioning is not well-understood by biologists today, the nutritional stress response in the bacterium *E. coli*. The application has led to biologically interesting results and has confirmed the importance of the refined qualitative abstraction.

The hybrid character of the dynamics of genetic regulatory networks has stimulated the interest in the application of hybrid-systems methods and tools over the past few years [3, 4, 5, 6, 7]. Our approach differs from this related work on several counts. Whereas we use piecewise-affine deterministic models, other groups have employed multi-affine deterministic models [3, 7] or stochastic models [6]. Without denying the interest of the latter approaches, we note that the class of models underlying our approach allows the qualitative analysis of high-dimensional systems, and is therefore well-adapted to state-of-the-art measurement techniques in molecular biology. The PADE models (1) in this paper have been well-studied in mathematical biology [1, 2], and have also formed the basis for other work in the field of hybrid systems [5]. However, the latter approach

does not take into account the dynamics of the system on threshold hyperplanes, where equilibrium points and other phenomena of interest may occur [16]. In addition, we use a tailored method for the computation of a qualitative PA transition system, instead of the generic quantifier elimination method used in [5]. This allows us to fully exploit the favorable mathematical properties of the PADE models (1), and thus promote the upscalability of the method to large and complex networks (Section 5), even when using a fine-grained partitioning of the phase space.

From a more general perspective, our approach can be seen as an application of the notion of discrete abstraction, introduced to study the dynamics of systems with an infinite number of states [17, 18]. Much work has focused on the identification of classes of continuous and discrete dynamical systems for which bisimulation relations with finite transition systems are guaranteed to exist. The results of this paper can be seen as showing that the weaker simulation relation may also be of considerable practical interest, especially for classes of systems for which the existence of a finite bisimulation cannot be guaranteed. Discrete abstraction criteria similar to the one used in this paper, based on the sign of the (higher) derivatives of continuous variables, have also been proposed by other authors in the fields of hybrids systems [23] and qualitative reasoning [24]. In comparison with these approaches, our work deals with a less general class of models. However, this allows the development and implementation of efficient, tailored algorithms for the practical computation of the qualitative dynamics of the system, even on (intersections of) threshold hyperplanes, where discontinuities may occur.

The possibility to use efficient algorithms for the computation of the qualitative PA transition system rests, to a large extent, on the approximation of the set $K(\boldsymbol{x})$ in (4) by the set $H(\boldsymbol{x})$ in (5). Because the latter set is hyperrectangular, the computation of domains, transitions, and sign patterns can be carried out seperately in every dimension, using the ordering of parameter values fixed by inequality constraints. Because $H(\boldsymbol{x})$ is an overapproximation of $K(\boldsymbol{x})$, the state transition graph may contain sequences of states that would not occur in the graph obtained by using $K(\boldsymbol{x})$. As a consequence, a PADE model may fail to be rejected by an observed time-series of measurements of the concentration variables. However, due to the fact that the approximation of $H(\boldsymbol{x})$ by $K(\boldsymbol{x})$ is conservative, a PADE model will never be falsely rejected. An obvious direction for further research would be to see whether finer approximations of $H(\boldsymbol{x})$ can be found that still allow tailored symbolic algorithms to be used that do not compromise the upscalability of the method to large and complex genetic regulatory networks.

References

1. Glass, L., Kauffman, S.: The logical analysis of continuous non-linear biochemical control networks. J. Theor. Biol. **39** (1973) 103–129
2. Thomas, R., d'Ari, R.: Biological Feedback. CRC Press (1990)

3. Belta, C., Finin, P., Habets, L., Halász, A., Imielinski, M., Kumar, V., Rubin, H.: Understanding the bacterial stringent response using reachability analysis of hybrid systems. In Alur, R., Pappas, G., eds.: Proc. HSCC 2004. LNCS 2993, Springer (2004) 111–125
4. de Jong, H., Gouzé, J.L., Hernandez, C., Page, M., Sari, T., Geiselmann, J.: Hybrid modeling and simulation of genetic regulatory networks: A qualitative approach. In Pnueli, A., Maler, O., eds.: Proc. HSCC 2003. LNCS 2623, Springer (2003) 267–282
5. Ghosh, R., Tomlin, C.: Symbolic reachable set computation of piecewise affine hybrid automata and its application to biological modeling: Delta-Notch protein signalling. Syst. Biol. **1** (2004) 170–183
6. Hu, J., Wu, W.C., Sastry, S.: Modeling subtilin production in *B. subtilis* using stochastic hybrid systems. In Alur, R., Pappas, G., eds.: Proc. HSCC 2004. LNCS 2993, Springer (2004) 417–431
7. Asarin, E., Dang, T.: Abstraction by projection and application to multi-affine systems. In Alur, R., Pappas, G., eds.: Proc. HSCC 2004. LNCS 2993, Springer (2004) 32–47
8. Lygeros, J., Pappas, G., Sastry, S.: An introduction to hybrid system modeling, analysis, and control. Preprints of 1st Nonlinear Control Network Pedagogical School, Greece (1999)
9. Antsaklis, P., Koutsoukos, X.: Hybrid dynamical systems: review and recent progress. In Samad, T., Balas, G., eds.: Software-enabled Control: Information Technologies for Dynamical Systems. Wiley-IEEE Press (2003)
10. de Jong, H.: Modeling and simulation of genetic regulatory systems: A literature review. J. Comput. Biol. **9** (2002) 69–105
11. de Jong, H., Gouzé, J.L., Hernandez, C., Page, M., Sari, T., Geiselmann, J.: Qualitative simulation of genetic regulatory networks using piecewise-linear models. Bull. Math. Biol. **66** (2004) 301–340
12. de Jong, H., Geiselmann, J., Hernandez, C., Page, M.: Genetic Network Analyzer: Qualitative simulation of genetic regulatory networks. Bioinformatics **19** (2003) 336–344
13. de Jong, H., Geiselmann, J., Batt, G., Hernandez, C., Page, M.: Qualitative simulation of the initiation of sporulation in *B. subtilis*. Bull. Math. Biol. **66** (2004) 261–300
14. Batt, G., de Jong, H., Geiselmann, J., Page, M., Ropers, D., Schneider, D.: Symbolic reachability analysis of genetic regulatory networks using qualitative abstraction. Technical report RR-5362 INRIA (2004)
15. Filippov, A.: Differential Equations with Discontinuous Righthand Sides. Kluwer Academic Publishers (1988)
16. Gouzé, J.L., Sari, T.: A class of piecewise linear differential equations arising in biological models. Dyn. Syst. **17** (2002) 299–316
17. Alur, R., Henzinger, T., Lafferriere, G., Pappas, G.: Discrete abstractions of hybrid systems. Proc. IEEE **88** (2000) 971–984
18. Chutinan, A., Krogh, B.: Verification of infinite-state dynamic systems using approximate quotient transition systems. IEEE Trans. Automat. Contr. **46** (2001) 1401–1410
19. Huisman, G., Siegele, D., Zambrano, M., Kolter, R.: Morphological and physiological changes during stationary phase. In Neidhardt *et al.* eds.: *E. coli* and *Salmonella*: Cellular and Molecular Biology. ASM Press (1996) 1672–1682.
20. Hengge-Aronis, R.: The general stress response in *E. coli*. In Storz, G., Hengge-Aronis, R., eds.: Bacterial Stress Responses. ASM Press (2000) 161–177

21. Ropers, D., de Jong, H., Page, M., Schneider, D., Geiselmann, H.: Qualitative simulation of nutritional stress response in *E. coli*. Technical Report RR-5412 (2004), submitted for publication
22. Batt, G., Bergamini, D., de Jong, H., Gavarel, H., Mateescu, R.: Model checking genetic regulatory networks using GNA and CADP. In Graf, S., Mounier, L., eds.: Proc. SPIN 2004. LNCS 2989, Springer (2004) 158–163
23. Tiwari, A., Khanna, G.: Series abstractions for hybrid automata. In Tomlin, C., Greenstreet, M., eds.: Proc. HSCC 2002. LNCS 2289, Springer (2002) 465–478
24. Kuipers, B.: Qualitative Reasoning: Modeling and Simulation with Incomplete Knowledge. MIT Press (1994)